Supplementary Information for

Interplay of hyporheic exchange and fine particle deposition in a riverbed

Guangqiu Jin[1,2], Yilin Chen[1,2], Hongwu Tang[1,2,#], Zhang Pei[1,3], Ling Li[4], D. A. Barry[5]

[1] State Key Laboratory of Hydrology-Water Resources and Hydraulic Engineering, Hohai University, Nanjing, China. Emails: jingq@hhu.edu.cn, hhucyl@hotmail.com, hwtang@hhu.edu.cn, peizhang.hhu@gmail.com, [2] Centre for Eco-Environmental Modelling, College of Water Conservancy and Hydropower Engineering, Hohai University, Nanjing, China, [3] School of Civil Engineering, University of Queensland, Queensland, Australia, [4] School of Engineering, Westlake University, Hangzhou, China. Email: liling@westlake.edu.cn, [5] Laboratoire de technologie écologique (ECOL), Institut d'ingénierie de l'environnement (IIE), Faculté de l'environnement naturel, architectural et construit (ENAC), Ecole Polytechnique Fédérale de Lausanne (EPFL), Station 2, 1015 Lausanne, Switzerland. Email: andrew.barry@epfl.ch

Content of this file

Table S1, Figures S1 to S4

Introduction

This supporting information includes results for $q_p(t=0)$, $ln(S/S_{max})$, permeability under different particle concentrations, pressure differences, particle diameters and collision efficiencies.

Table S1 Values for $q_p(t=0)$ under different cases

$\boldsymbol{q_p(t=0)}$	Value (kg/s)
Base case	3.48×10^{-7}
$\boldsymbol{C_0 = 4\ \mathrm{kg/m^3}}$	2.71×10^{-6}
$\boldsymbol{C_0 = 8\ \mathrm{kg/m^3}}$	7.92×10^{-6}
$\boldsymbol{h_m = 2.38 \times 10^{-4}\ \mathrm{m}}$	2.07×10^{-7}
$\boldsymbol{h_m = 6.44 \times 10^{-4}\ \mathrm{m}}$	5.15×10^{-7}
$\boldsymbol{d_p = 4\ \mathrm{um}}$	2.25×10^{-6}
$\boldsymbol{d_p = 8\ \mathrm{um}}$	8.74×10^{-6}
$\boldsymbol{\alpha = 0.2}$	3.44×10^{-7}
$\boldsymbol{\alpha = 0.6}$	3.39×10^{-7}

(a)

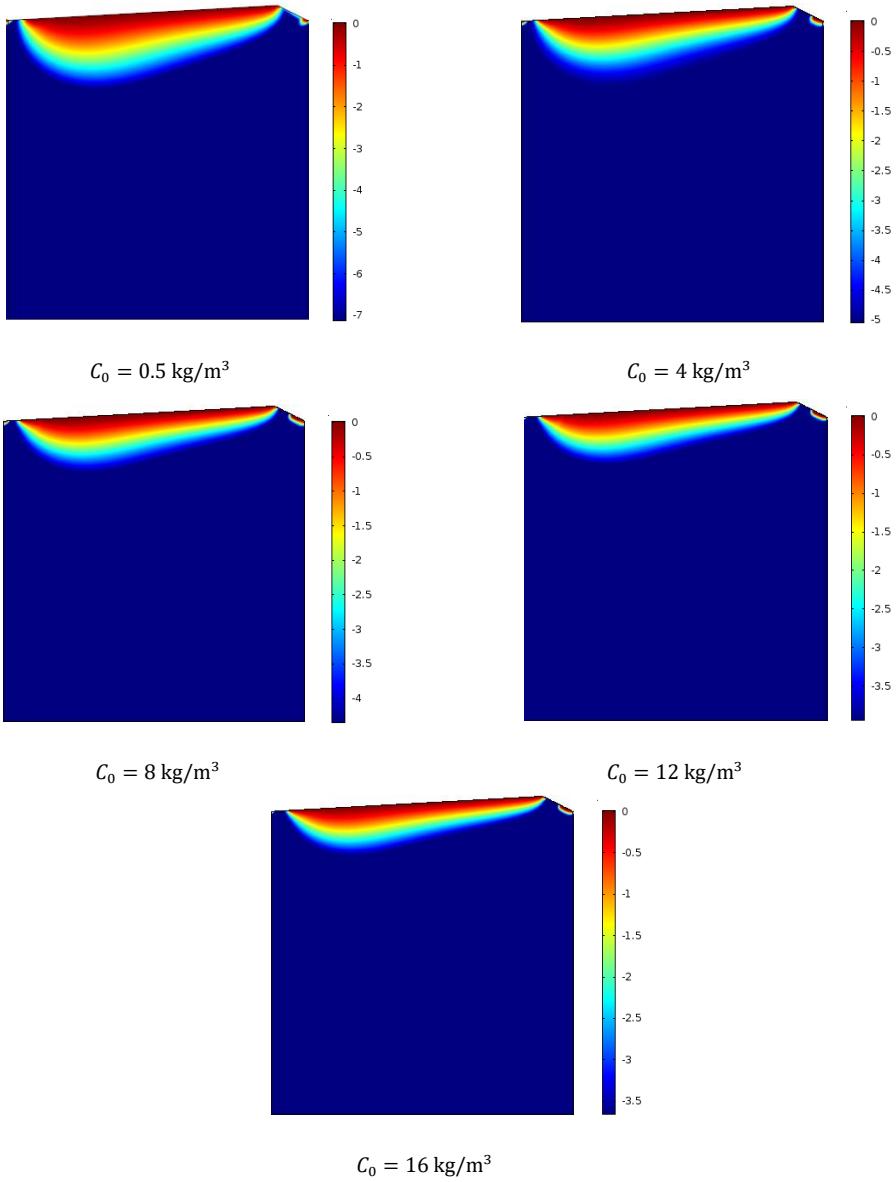
$C_0 = 0.5$ kg/m³
$C_0 = 4$ kg/m³
$C_0 = 8$ kg/m³
$C_0 = 12$ kg/m³
$C_0 = 16$ kg/m³

(b)

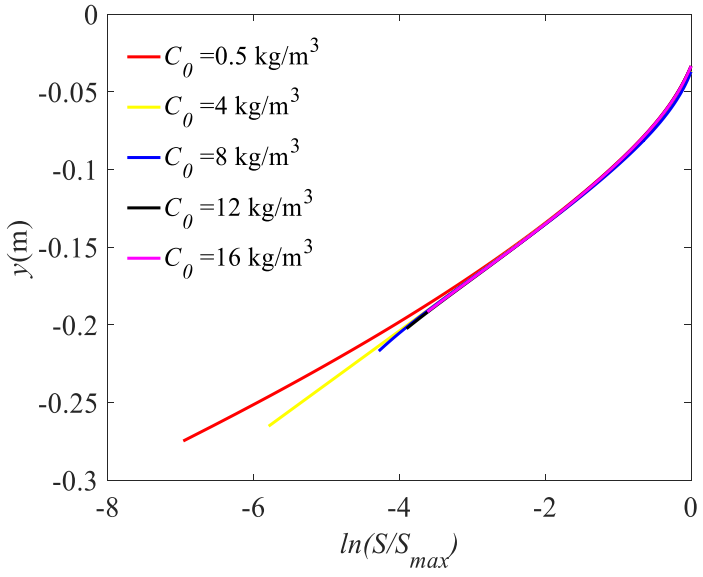
C_0 =0.5 kg/m³
C_0 =4 kg/m³
C_0 =8 kg/m³
C_0 =12 kg/m³
C_0 =16 kg/m³
y(m)
ln(S/S_max)

(c)

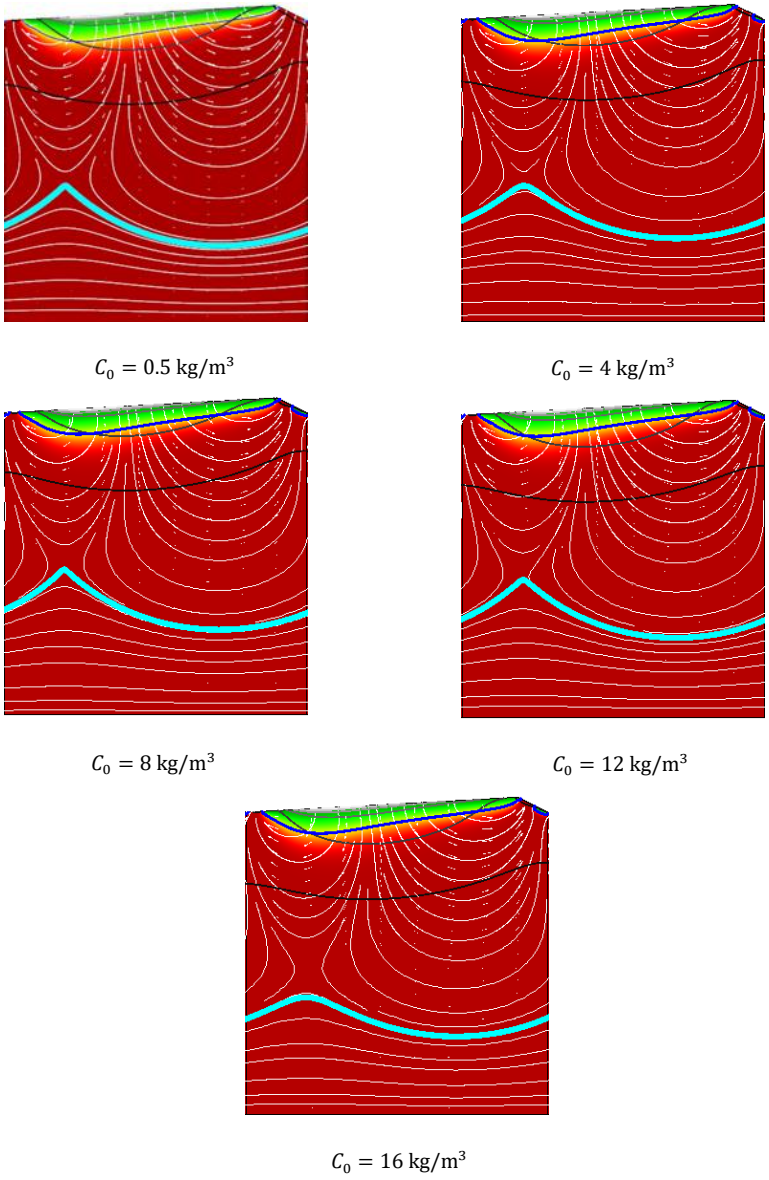

Figure S1 (a) Distribution of $ln(S/S_{max})$ in the riverbed when t=58333.33 h. (b) Distribution of $ln(S/S_{max})$ along the cutline L as shown in Figure 5. (c) Riverbed permeability distribution in the steady state (t= 58333.33 h) under different particle concentrations. The legend is the same as that in Figure 5.

(a)

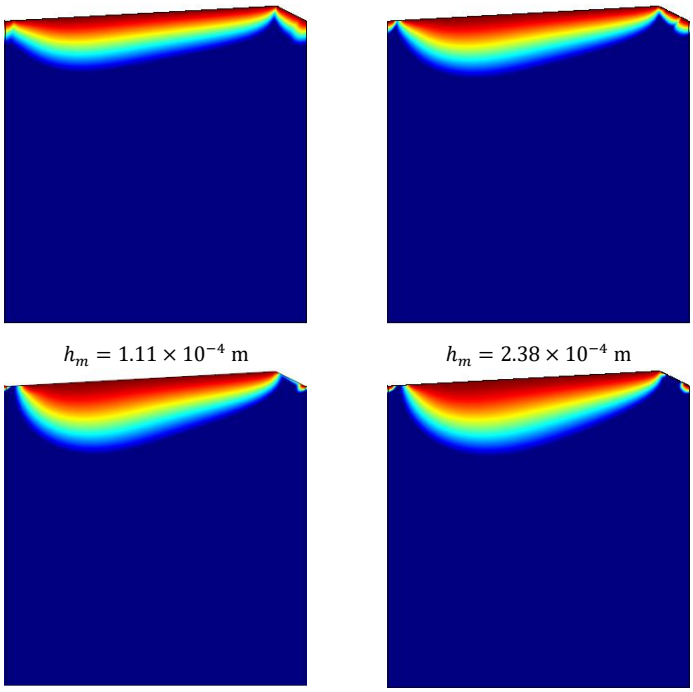
$h_m = 1.11 \times 10^{-4}$ m
$h_m = 2.38 \times 10^{-4}$ m
$h_m = 4.75 \times 10^{-4}$ m
$h_m = 6.44 \times 10^{-4}$ m

(b)

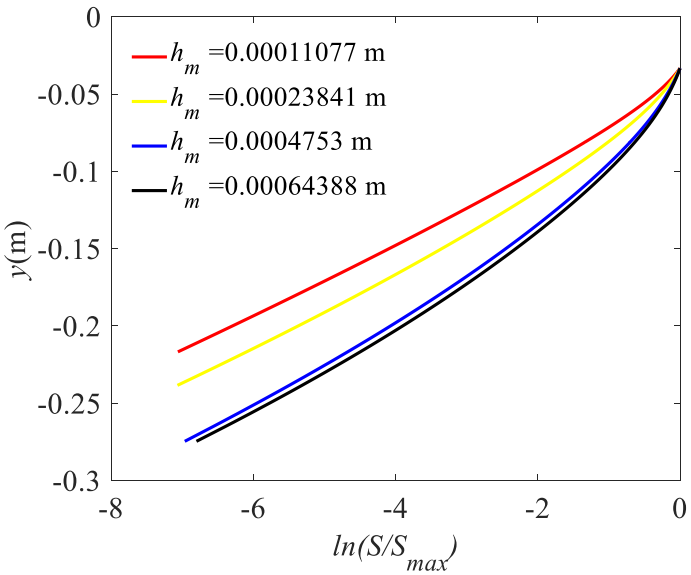
h_m =0.00011077 m
h_m =0.00023841 m
h_m =0.0004753 m
h_m =0.00064388 m
0
-0.05
-0.1
-0.15
-0.2
-0.25
-0.3
y(m)
-8
-6
-4
-2
0
$ln(S/S_{max})$

(c)

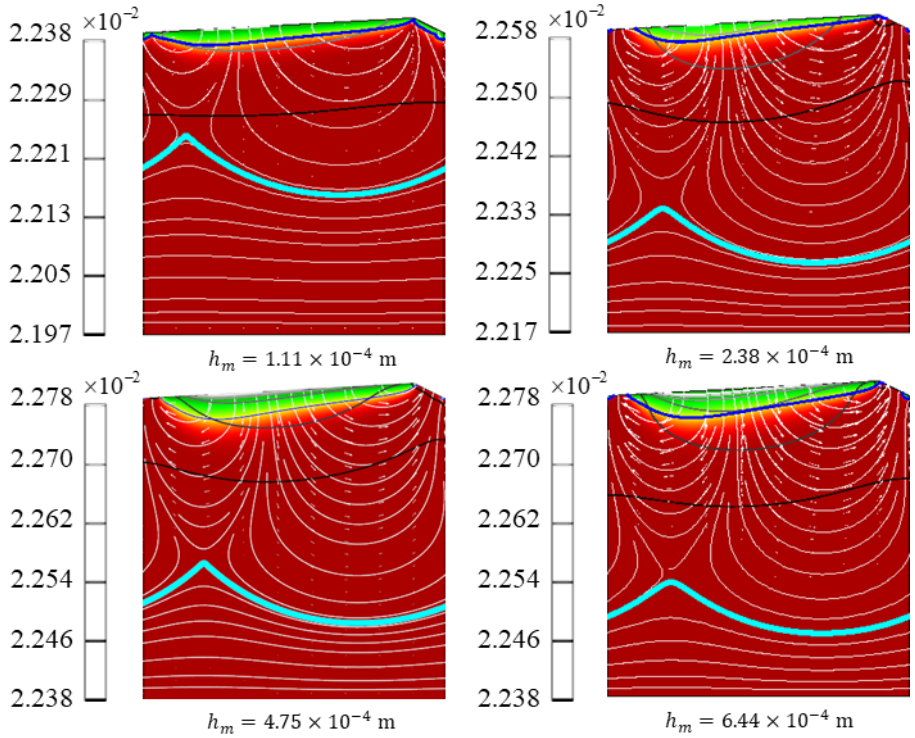

Figure S2 (a) Distribution of $ln(S/S_{max})$ in the riverbed when t=58333.33 h. (b) Distribution of $ln(S/S_{max})$ along the cutline L as shown in Figure 5. (c) Riverbed permeability distribution in the steady state (t= 58333.33 h) under different pressure difference, the legend of permeability is the same as Figure 5. The legend of hydraulic head is shown on each case's left hand side.

(a)

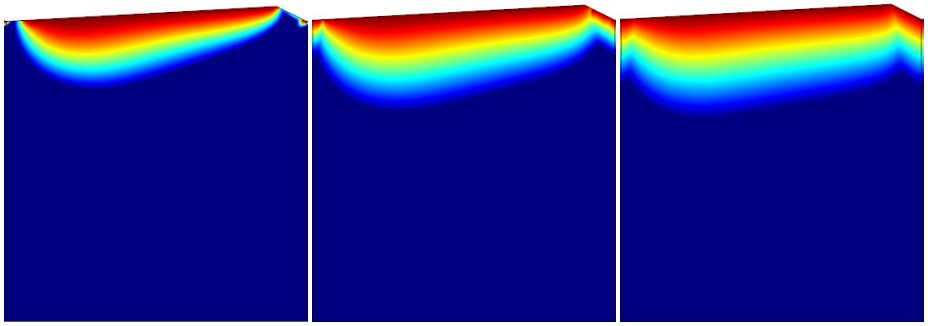

$d_p = 1\mu m$ $d_p = 2\mu m$ $d_p = 3\mu m$

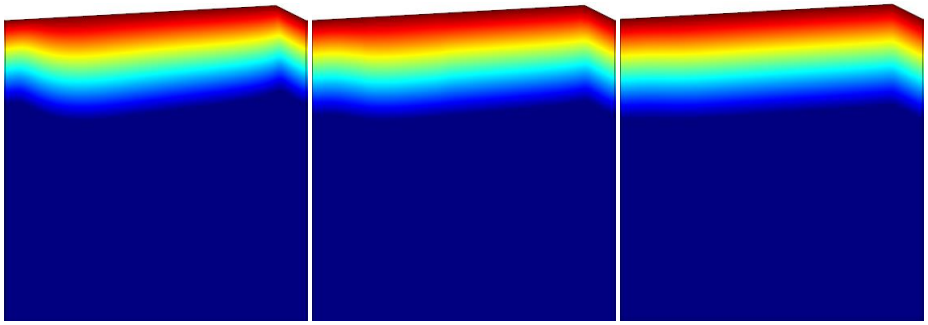

$d_p = 4\mu m$ $d_p = 6\mu m$ $d_p = 10\mu m$

(b)

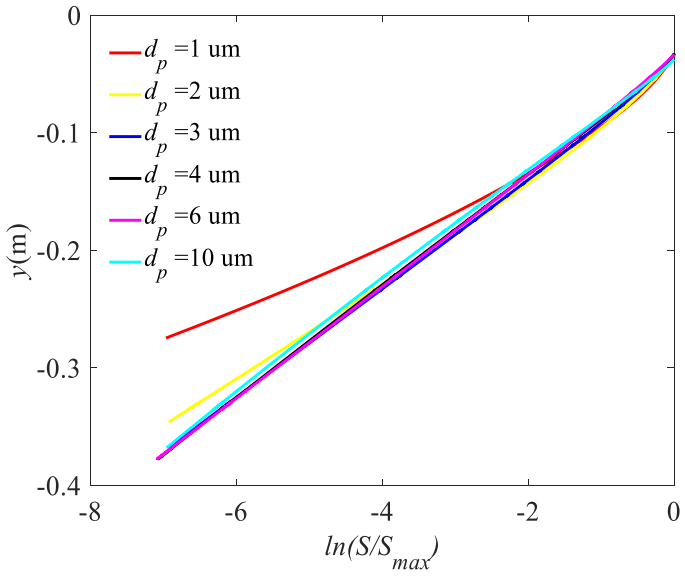

c)

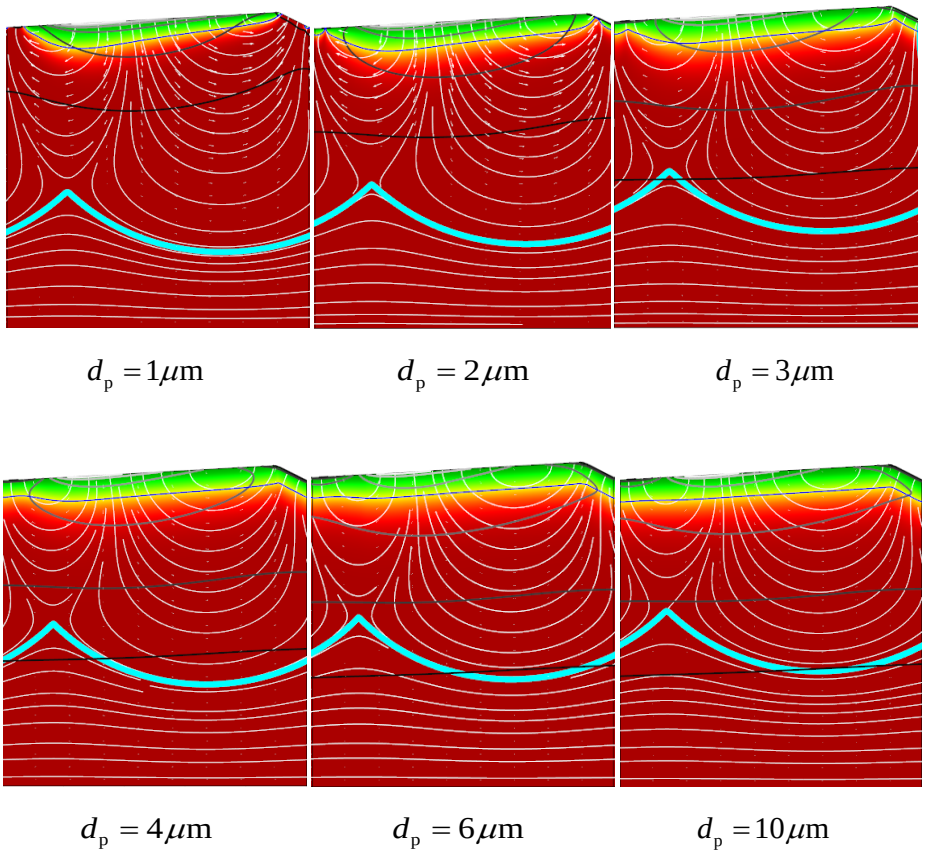

Figure S3 (a) Distribution of $ln(S/S_{max})$ in the riverbed when t=58333.33 h, legend is the same as Fig. 5. (b) Distribution of $ln(S/S_{max})$ along the cutline L as shown in Figure 5. (c) Riverbed permeability distribution in the steady state (t= 58333.33 h) under different particle diameters. The legend is the same as that in Fig. 5.

a)

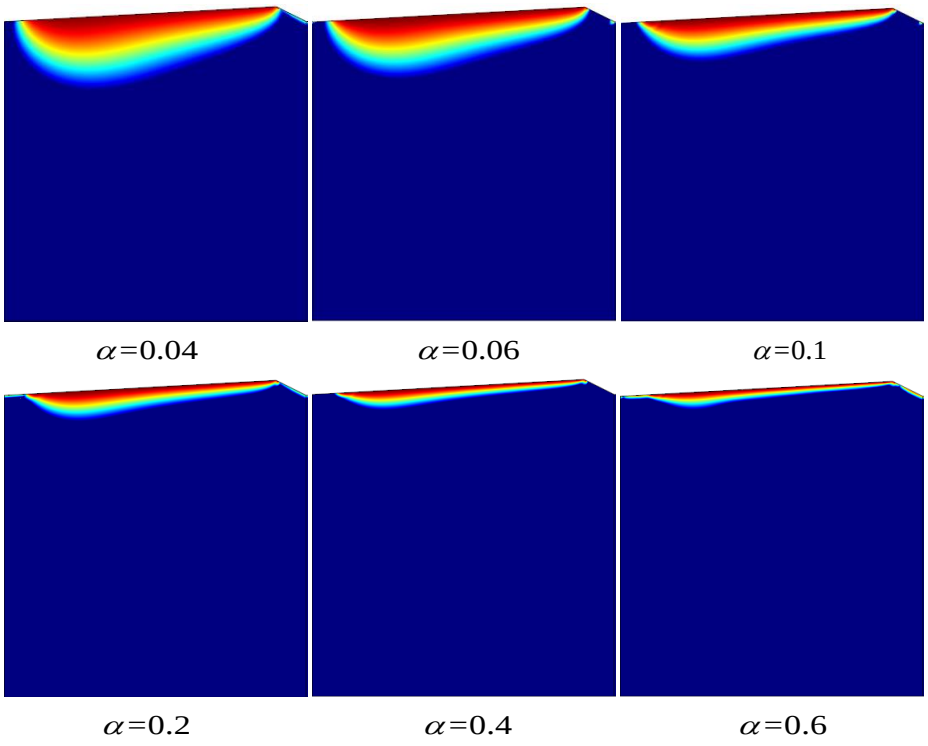
α=0.04
α=0.06
α=0.1
α=0.2
α=0.4
α=0.6

b)

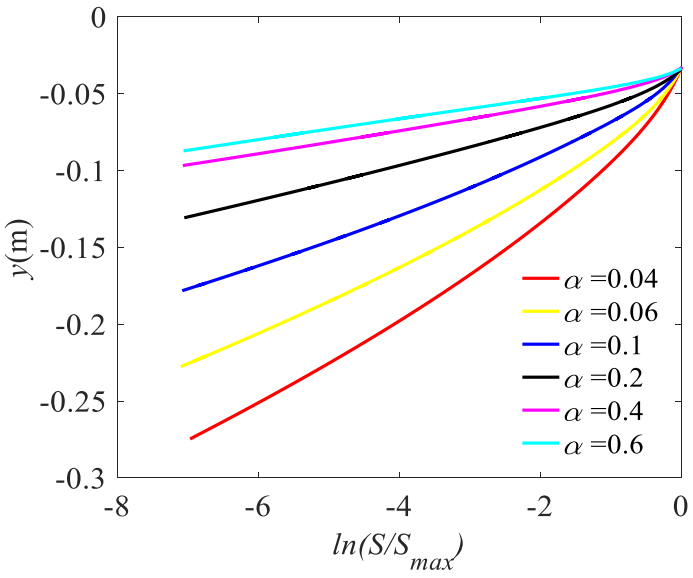
0
-0.05
-0.1
-0.15
-0.2
-0.25
-0.3
y(m)
-8
-6
-4
-2
0
ln(S/S_max)
α =0.04
α =0.06
α =0.1
α =0.2
α =0.4
α =0.6

c)

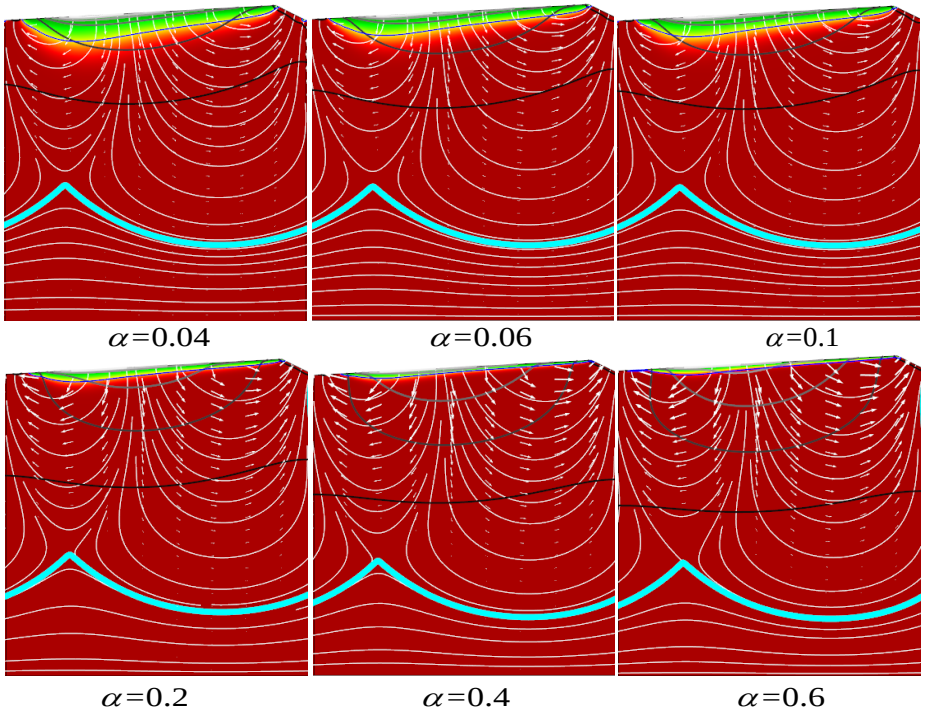

Figure S4 (a) Distribution of $ln(S/S_{max})$ in the riverbed when t=58333.33 h, the legend is the same as Figure 5. (b) Distribution of $ln(S/S_{max})$ along the cutline L as shown in Figure 5. (c) Riverbed permeability distribution in the steady state (t= 58333.33 h) under different sediment collision efficiencies. The legend is the same as that in Figure 5.